Current Biology 21, 1960–1967, December 6, 2011 ©2011 Elsevier Ltd All rights reserved DOI 10.1016/j.cub.2011.10.050

Article

A $G\alpha_q$-Ca^{2+} Signaling Pathway Promotes Actin-Mediated Epidermal Wound Closure in *C. elegans*

Suhong Xu[1] and Andrew D. Chisholm[1,*]
[1]Section of Cell and Developmental Biology, Division of Biological Sciences, University of California San Diego, 9500 Gilman Drive, La Jolla, CA 92093, USA

Summary

Background: Repair of skin wounds is essential for animals to survive in a harsh environment, yet the signaling pathways initiating wound repair in vivo remain little understood. In *Caenorhabditis elegans*, a p38 mitogen-activated protein kinase (MAPK) cascade promotes innate immune responses to wounding but is not required for other aspects of wound healing. We therefore set out to identify additional wound response pathways in *C. elegans* epidermis.
Results: We show here that wounding the adult *C. elegans* skin triggers a rapid and sustained rise in epidermal Ca^{2+} that is critical for survival after wounding. The wound-triggered rise in Ca^{2+} requires the epidermal transient receptor potential channel, melastatin family (TRPM) channel GTL-2 and IP_3R-stimulated release from internal stores. We identify an epidermal signal transduction pathway that includes the $G\alpha_q$ EGL-30 and its effector PLCβ EGL-8. Loss of function in this pathway impairs survival after wounding. The $G\alpha_q$-Ca^{2+} pathway is not required for known innate immune responses to wounding but instead promotes actin-dependent wound closure. Wound closure requires the Cdc42 small GTPase and Arp2/3-dependent actin polymerization and is negatively regulated by Rho and nonmuscle myosin. Finally, we show that the death-associated protein kinase DAPK-1 acts as a negative regulator of wound closure.
Conclusions: Skin wounding in *C. elegans* triggers a Ca^{2+}-dependent signaling cascade that promotes wound closure, in parallel to the innate immune response to damage. Wound closure requires actin polymerization and is negatively regulated by nonmuscle myosin.

Introduction

All organisms must repair damage caused by mechanical injury or environmental pathogens. The skin in particular exhibits a complex sequence of wound healing processes [1]. Understanding the molecular basis of wound healing is of increasing relevance to human health as chronic or nonhealing wounds become more common in the elderly or in diabetic individuals [2]. Several vertebrate and invertebrate models are being explored for molecular genetic analyses of wound healing [3–5]. Importantly, transcription factors involved in epidermal wound healing show evolutionary conservation [6, 7], suggesting that mechanisms in wound healing could share significant similarity.

Despite extensive efforts in the analysis of wound healing, many questions remain open. It is not well understood how barrier epithelia detect damage nor how the initial sensation of damage is transmitted to develop a coordinated wound healing response. Studies in *Drosophila* wound healing have highlighted the role of epidermal tyrosine kinases and ERK signaling in early wound responses [8, 9], whereas mammalian wound responses appear to be initiated by a variety of growth factors and cytokines [10].

The epidermis of the nematode *Caenorhabditis elegans* is a simple barrier epithelium that generates an external cuticle. The nematode body is under hydrostatic pressure, so puncture wounds can be fatal if not repaired. Such wounds may be common in nature, where nematodes encounter damaging substrates and cuticle-puncturing pathogens [11, 12]. Needle or laser wounding of the epidermis triggers a p38 mitogen-activated protein kinase (MAPK)/PMK-1 cascade that activates transcription of antimicrobial peptide genes [13]. This innate immune response defends against opportunistic infection at wounds, because p38 MAPK mutants display reduced survival after wounding [14]. However, the p38 MAPK cascade is not required for other wound repair processes such as scar formation [14].

To address how other aspects of *C. elegans* wound healing are activated, we have examined other known wound-triggered pathways. Ca^{2+} is important for embryonic wound healing [15] and in wound responses of single cells [16]. However, the in vivo role of Ca^{2+} signals in repair of mature barrier epithelia has been less clear. We show here that Ca^{2+} signals are critical for *C. elegans* wound healing, acting in parallel to innate immune response pathways to promote actin rearrangement during wound closure. Unlike embryonic or single-cell wounds, which typically involve actomyosin purse-string-based contractility [17], we find that wounds in the adult *C. elegans* skin close by an actin-polymerization-based mechanism negatively regulated by nonmuscle myosin.

Results

Wounding Triggers a Rapid and Sustained Rise in Epidermal Ca^{2+}

To visualize Ca^{2+} dynamics in the epidermis after wounding, we expressed the Ca^{2+} sensor GCaMP3 [18] under the control of epidermal-specific promoters (see Experimental Procedures; see also Table S1 available online). The adult *C. elegans* epidermis consists of seam cells and multinucleate syncytial cells, of which hyp7 is the largest. Needle wounding of the syncytial hyp7 epidermis in late larvae or adults triggered increases in epidermal GCaMP fluorescence that spread from the site of injury to approximately 1/3 the length of the animal (Movie S1; Figure 1A). To quantitate wound-triggered Ca^{2+} dynamics, we performed localized laser wounding and imaged epidermal GCaMP using spinning-disk microscopy (Movie S2: Figures 1B and 1C). Laser wounding triggered increases in GCaMP fluorescence similar to those seen after needle wounding; GCaMP waves traveled at 25.6 ± 2 $\mu m\ s^{-1}$ (Figure S1A), a speed consistent with propagation via Ca^{2+}-induced Ca^{2+} release from internal stores. Thereafter, elevated GCaMP fluorescence underwent small global oscillations but was otherwise stable, and typically persisted for >1 hr before declining (Movie S3; Figure 1D).

*Correspondence: chisholm@ucsd.edu

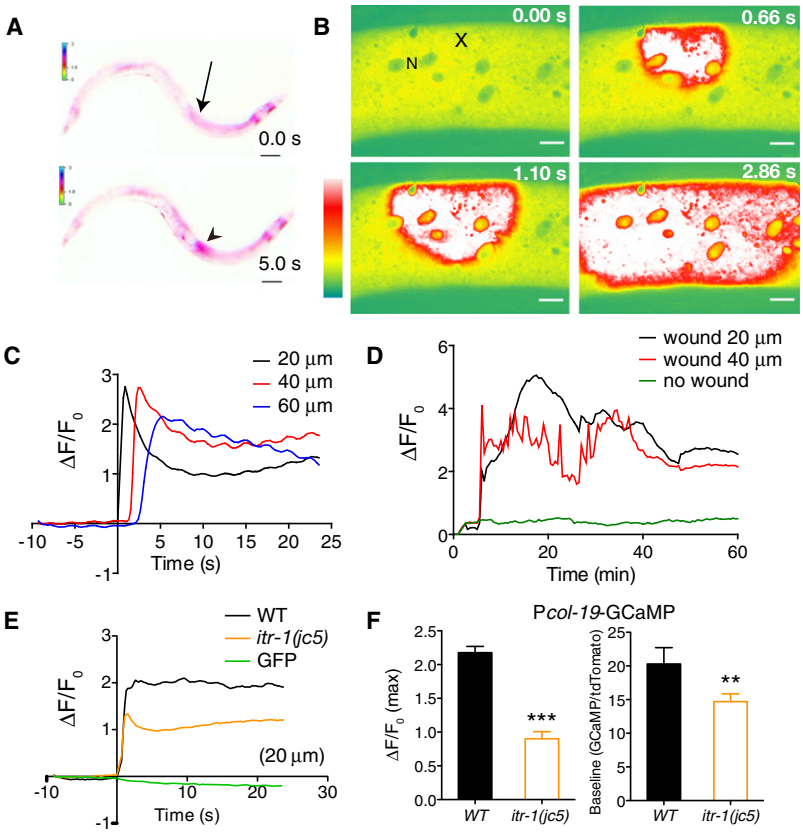

Figure 1. Wounding Triggers an Epidermal Ca^{2+} Response

(A) Epidermal GCaMP induction after needle wounding; P*col-19*-GCaMP (*juIs319*). The site of wounding is indicated by arrow; the GCaMP fluorescence increase is marked by an arrowhead (see also Movie S1); inverted color scale.

(B) Epidermal GCaMP fluorescence levels after femtosecond laser wounding. Image of lateral view of epidermis in midbody; x marks site of laser wound; N, epidermal nucleus. Images are from spinning disk confocal, intensity coded. See also Movie S2.

(C) Quantitation of GCaMP $\Delta F/F_0$ at 20, 40, and 60 µm from wound site; representative trace. Note oscillations in GCaMP levels.

(D) Prolonged elevation of epidermal GCaMP fluorescence after wounding; representative trace, from Movie S3 at positions 20 and 40 µm from wound site. Unwounded animals display minimal variation in GCaMP signals (green line).

(E) *itr-1(jc5cs)* mutants cultured at 15°C display reduced GCaMP $\Delta F/F_0$ compared to wild-type (WT) (average traces); wounding does not affect epidermal GFP fluorescence (green line, E).

(F) *itr-1* mutants display reduced peak $\Delta F/F_0$ after wounding and reduced baseline GCaMP fluorescence, measured as ratio to epidermally expressed tdTomato. n > 20 per genotype. Scale bars represent 100 µm (A) and 10 µm (B).

To test whether release from internal stores contributed to the epidermal Ca^{2+} wave, we tested the IP_3 receptor ITR-1. *itr-1(jc5cs)* mutants displayed significantly reduced epidermal GCaMP responses to injury (Figures 1E and 1F). To reduce IP_3 signaling specifically in the epidermis, we overexpressed N-terminal IP_3 binding domains ("IP_3 sponges") [19]. Expression of IP_3 sponges in the adult epidermis reduced both baseline and wound-induced increase in GCaMP fluorescence (Figures S1B and S1C), indicating that wounding triggers Ca^{2+} release from internal stores in the epidermis.

An Epidermal TRPM Channel Is Required for Ca^{2+} Responses

Release of Ca^{2+} from internal stores could be triggered by an initial Ca^{2+} influx across the epidermal cell membrane or by other signals that activate the IP_3R. To define the sources of epidermal Ca^{2+}, we screened known Ca^{2+} channels and Ca^{2+} signaling components (Table S2). *C. elegans* encodes >50 Ca^{2+} channel subunits, including 17 divalent cation channels in the TRP class [20]. Several TRP channels are expressed in the epidermis, including the transient receptor potential channel, melastatin family (TRPM) channel GTL-2 [21]. Of 11 TRP channels tested, only GTL-2 was required for normal epidermal Ca^{2+} responses (Figures 2A and 2B). Epidermal expression of GTL-2 rescued *gtl-2* Ca^{2+} defects (Figure 2B), whereas muscle- or neuron-specific expression did not rescue (data not shown), suggesting that GTL-2 can act cell autonomously in epidermal Ca^{2+} homeostasis. GTL-2 is localized to the plasma membrane in the epidermis [21], suggesting that GTL-2 may affect initial influx of Ca^{2+} after wounding rather than subsequent calcium-induced Ca^{2+} release.

Epidermal Ca^{2+} Responses Are Required for Survival of Wounding

To address the importance of Ca^{2+} and GTL-2 in wound healing, we analyzed survival postwounding. We measured survival 24 hr after needle wounding, a time when >90% of wounded wild-type (WT) animals are healthy [14]. *gtl-2* mutants showed drastically reduced survival postwounding, a phenotype rescued by epidermal expression of GTL-2, suggesting that epidermal GTL-2 is required for survival after wounding (Figure 2C). Expression of IP_3 sponges in the epidermis caused smaller decreases in survival, consistent with their partial reduction in epidermal Ca^{2+} (Figure S1D). Loss of function in other TRPM family members GON-2 or GTL-1 can compensate for loss of GTL-2 function via systemic ion homeostasis [21, 22], and indeed *gtl-2 gon-2* or *gtl-2 gtl-1* double mutants showed restored viability after wounding (Figure S2B). These observations further support the model that GTL-2 contributes to epidermal Ca^{2+} homeostasis required for wound responses.

Reduced survival after wounding could reflect poor overall health rather than a defect in wound repair. To address whether developmental defects might account for reduced survival after wounding, we used tissue- and stage-specific RNA interference (RNAi) to reduce gene function only in the adult epidermis (see Experimental Procedures). Adult epidermal-specific RNAi of genes acting in the epidermal innate immune response, including the Toll/Interleukin receptor adaptor domain gene *tir-1* [23], reduced postwound survival (Figure 2F), indicating effective gene knockdown in this strain. Adult epidermal-specific RNAi of Ca^{2+} signaling genes, including *itr-1* and *gtl-2*, significantly reduced postwound survival (Figure 2F), confirming that ITR-1 and GTL-2 are required cell autonomously for survival after epidermal wounding.

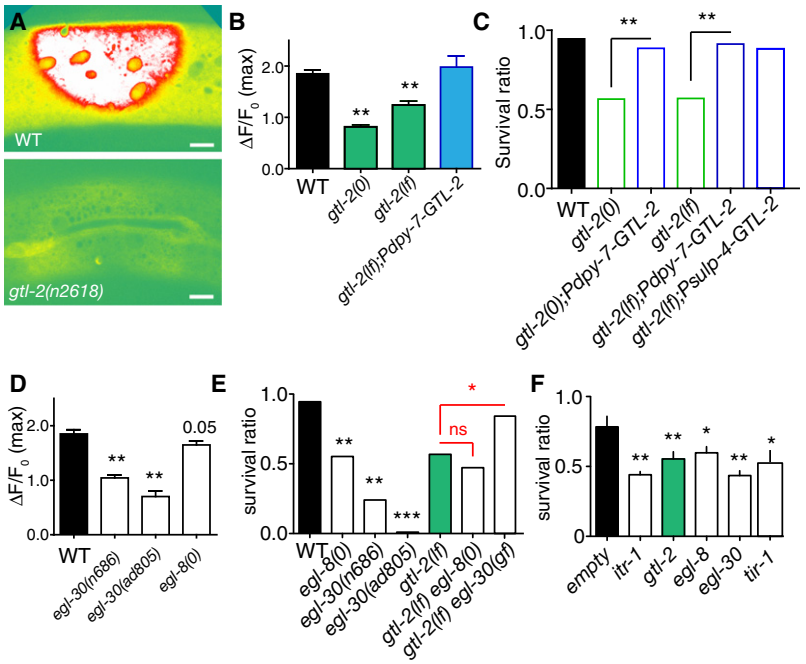

Figure 2. TRPM Channel GTL-2 and Gαq/PLCβ Signaling Are Required for Epidermal Ca^{2+} Responses and Survival after Wounding

(A) Epidermal Ca^{2+} responses to wounding are reduced in *gtl-2* mutants; imaged of P*col-19*-GCaMP(*juIs319*) (1 s after laser wound). Scale bars represent 10 μm.

(B) Quantitation of peak $\Delta F/F_0$ in *gtl-2(0)* null mutants (*tm1463*) and *gtl-2(lf)* partial loss of function *n2618* mutants; rescue by expression of GTL-2 under epidermal control (*juEx2893*). n > 30 per genotype.

(C) *gtl-2* mutants display reduced survival after wounding; rescue by GTL-2::GFP expressed under control of epidermal (P*dpy-7*, *juEx2893*) or excretory system (P*sulp-4*, *juEx3216*) promoters. GTL-2::GFP signals are weak and do not interfere with GCaMP imaging. Survival ratio calculated as fraction of animals alive 24 hr post-wounding/number unwounded alive; n > 100 per genotype.

(D) Partial loss of function in *egl-30* strongly reduces epidermal baseline Ca^{2+} and $\Delta F/F_0$; loss of function in *egl-8* reduces baseline GCaMP signal and has a small effect on $\Delta F/F_0$; n > 50 per genotype.

(E) Reduced survival of *egl-8* and *egl-30* mutants post-wounding; *egl-8(0) gtl-2(lf)* double mutants are not further enhanced; n > 500 per genotype. *egl-30(gf)* suppresses survival defects of *gtl-2* in double mutants.

(F) Epidermal-specific RNAi of *egl-8* and *egl-30* significantly reduces survival postwounding, comparably to RNAi of *itr-1* or *gtl-2*; n > 200 per RNAi. All bar charts show mean ± SEM. For statistical analysis, we used Student's t test (B), Mann-Whitney test (D and F), or Fisher's exact test (C and E); ***p < 0.001, **p < 0.01; *p < 0.05; ns, not significant.

$G\alpha_q$ Signaling Is Required for the Epidermal Ca^{2+} Response to Wounding

Among genes required for normal Ca^{2+} levels in the epidermis we identified *egl-8*, which encodes phospholipase Cβ and *egl-30*, encoding the regulatory $G\alpha_q$ protein for EGL-8. *egl-8* and *egl-30* mutants both displayed reduced epidermal Ca^{2+} (Figure 2D; Figure S2A) and impaired survival postwounding (Figure 2E). *egl-8* null mutants did not enhance *gtl-2(lf)* survival phenotypes (Figure 2E), suggesting that *egl-8* and *gtl-2* act in a common pathway. *egl-30* null mutants arrest during larval development, precluding firm conclusions from double mutants. However, a gain of function mutation, *egl-30(js126)*, significantly suppressed survival defects of *gtl-2(lf)* mutants, consistent with EGL-30 acting downstream or in parallel to GTL-2. As PLCβ generates IP_3 in response to G protein couple receptor (GPCR) signals, these results suggest EGL-30 and PLCβ promote epidermal Ca^{2+} release via ITR-1 after wounding.

EGL-30 is expressed in many tissues, including the epidermis [24], whereas EGL-8 expression has been predominantly observed in neurons. We found that epidermal-specific RNAi of *egl-8* or *egl-30* significantly reduced postwounding survival without affecting other behaviors such as egg-laying (Figure 2F; data not shown). Conversely, epidermal-specific expression of EGL-8 was sufficient to rescue postwound survival defects of *egl-8* mutants but did not rescue their Egl phenotypes (data not shown). We conclude that the EGL-30/EGL-8 pathway functions within the epidermis to promote wound responses.

Ca^{2+} Signals Are Not Involved in the Known Innate Immune Responses to Wounding

Sterile wounding activates an epidermal TIR-1/PMK-1 p38 MAPK cascade that induces epidermal expression of antimicrobial peptides (AMPs) such as *nlp-29* [13]. Wounding also induces p38-independent transcription of caenacin-type (*cnc*) AMPs via the SMA-6 TGFβ receptor [25]. We tested whether Ca^{2+} signaling might intersect with these pathways and found that loss of function in *gtl-2* or *egl-30* had no effect on induction of *nlp-29* or *nlp-30* (Figures 3A and 3B). *egl-8* null mutants also displayed normal AMP induction, consistent with previous results on *egl-8(n488)* [26]. *gtl-2* and *egl-30* mutants also showed normal induction of *cnc-1* and *cnc-2* after wounding (Figure 3B). These findings suggest that $G\alpha_q/Ca^{2+}$ signals act in parallel to immune responses to wounding. Conversely, loss of function in the TIR-1/PMK-1 pathway or in $G\alpha_{12}$/GPA-12 did not affect epidermal Ca^{2+} (Figures S3A and S3B). Double mutants between *gtl-2* or *egl-8* and *tir-1* or *pmk-1* displayed additive or synergistic reductions in survival after wounding (Figure 3C). Taken together, these results suggest that epidermal Ca^{2+} and innate immune responses act in parallel to promote survival after wounding.

Ca^{2+} Signals Trigger Formation of Actin Rings at Wounds

We next asked whether the need for Ca^{2+} signaling in survival of wounding reflected defects in specific repair processes. Healing of adult wounds typically involves cell proliferation, migration and reepithelialization by cell crawling, and remodeling of extracellular matrix (ECM). In contrast, wound closure in embryonic epithelia is characterized by contractile actomyosin cables ("purse strings") [27, 28]. Further, actin [29] cable formation in *Xenopus* oocyte wound closure is Ca^{2+} dependent [30]. We therefore focused on whether Ca^{2+} signals promoted cytoskeletal dynamics in wound closure. To visualize the epidermal actin cytoskeleton, we expressed the F-actin marker GFP-moesin [31] in the epidermis. GFP-moesin distribution in the unwounded epidermis was diffuse (Figure 4A). Within minutes of needle wounding, a dense ring of filamentous GFP indicative of actin filaments formed at the site of damage (Movie S4; Figure 4A). In most cases, the actin ring gradually closed over the next 1–2 hr; a minority failed to close over this time period, possibly reflecting variability in

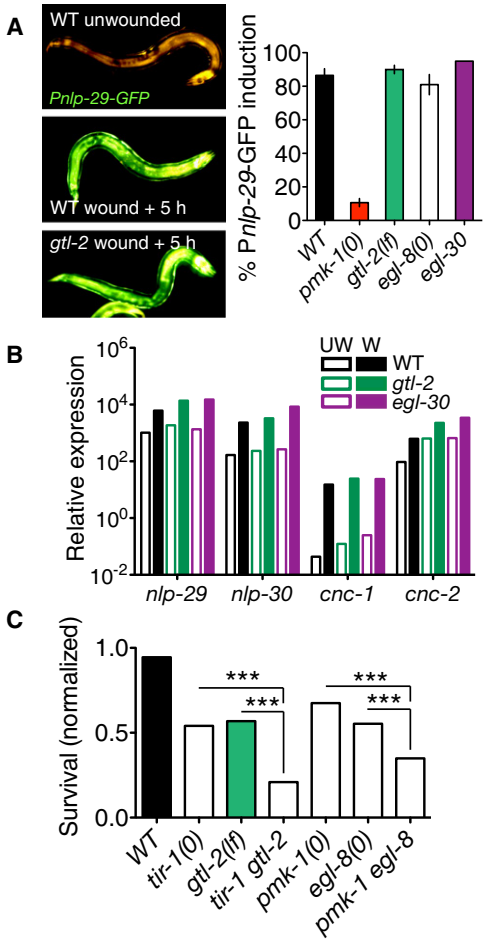

Figure 3. Epidermal Ca^{2+} Signals Act in Parallel to Known Innate Immune Pathways

(A) Representative images (WT unwounded, WT wounded + 5 hr and *gtl-2* wounded + 5 hr) and quantitation of P*nlp-29*-GFP(*frIs7*) induction after needle wounding; n > 100 per genotype.

(B) *gtl-2(n2618)* and *egl-30(n686)* mutants displayed normal basal levels (UW, empty bars) and wound-induced levels (W, filled bars) of epidermal antimicrobial peptide transcripts; RNA extracted from ~50 animals 6 hr after needle wounding. Expression levels are relative to *ama-1* in multiple quantitative RT-PCRs.

(C) Loss of function in Ca^{2+} signaling genes and in innate immune response genes has additive or synergistic effects on postwounding survival. n > 300 per genotype. Statistical analysis used Fisher's exact test.

needle wounding or in closure dynamics. After 24 hr, the actin rings were completely closed (Figure 4B) and colocalized with autofluorescent scar material [13]. These findings suggest that *C. elegans* adult wound closure involves a dynamic rearrangement of the actin cytoskeleton.

To quantitate the dynamics of actin during wound closure, we used line scans of confocal images to measure the GFP-moesin ring diameter at 1 hr after wounding, a time intermediate in the closure process (Figures 4C and 4D). We first tested whether Ca^{2+} signals promote closure by incubating wounded worms in Ca^{2+} chelators such as BAPTA-AM and found that these treatments severely compromised actin ring formation (Figure 4C). Incubation in Ca^{2+} chelators also reduced survival postwounding (Figure S1E). *gtl-2* mutants displayed reduced actin accumulation after wounding and impaired closure of actin rings (Figures 4C and 4D; Movie S4). Incubation of *gtl-2* mutants in media containing increased external Ca^{2+} significantly restored closure (Figures 4C and 4D), suggesting that the closure defects of *gtl-2* mutants result from reduced epidermal Ca^{2+}. Conversely, mutants defective in innate immune responses (*tir-1, pmk-1*) displayed normal actin ring formation (Figure S3C). The reduced survival of immunocompromised mutants such as *tir-1* can be partly suppressed by incubation with antibiotics or DNA replication blockers such as 5-fluoro-2′-deoxuridine (FUDR) [14]. In contrast, impaired survival of *gtl-2* or *egl-8* mutants was not suppressed by FUDR (Figure S2C), consistent with a defect in physical closure of wounds.

Wound Closure Involves Local Actin Polymerization and Is Inhibited by Nonmuscle Myosin

The dynamics of actin rings after wounding suggest that wound closure involves the actin cytoskeleton but do not distinguish whether this is driven by actomyosin-based contractility or some other form of actin dynamics. Time-lapse analysis of actin wounding suggested that at least two processes contribute to actin dynamics: first, recruitment of F-actin to the ring, and second, closure of the ring. To address the role of actin, we first tested actin polymerization inhibitors. Incubation of animals in the actin polymerization inhibitor Latrunculin A (LatA) completely blocked recruitment of actin to wounds (Figure S4A) and significantly reduced postwounding survival (Figure S4B), indicating that actin polymerization is essential for formation of actin rings.

We next used RNAi to test the roles of known regulators of actin polymerization, including Rho-family GTPases and a set of actin binding or nucleating proteins. Among small GTPases, Rho is required for actin cable formation in wound closure [32], whereas Cdc42 is essential for actin assembly and disassembly in several contexts, including filopodial protrusions [33]. We found that *cdc-42(RNAi)* abolished actin recruitment to wound sites, whereas loss of function in *rho-1* caused actin rings to close more rapidly than in the WT. In contrast, loss of function in the Rac genes (*rac-2, ced-10, mig-2*) had little effect on actin recruitment or survival (data not shown). Knockdown of the actin nucleation factors WSP-1/WASP or ARX-2/Arp2/3 complex reduced but did not abolish ring closure (Figures 5A and 5B); *arx-2(RNAi)* strongly reduced survival postwounding (Figure 5C). Taken together, these results suggest that Cdc42-dependent actin polymerization is important for wound closure and survival.

Finally, to test whether *C. elegans* wound closure required actomyosin contractility, we reduced the function of nonmuscle myosin. *C. elegans* encodes two nonmuscle myosin heavy chains, NMY-1 and NMY-2, with partly redundant functions in epidermal development [34]. Unexpectedly, loss of function in either *nmy* gene significantly promoted actin ring closure (Figures 6A and 6B; Movie S5), as did RNAi of the epidermally expressed myosin light chain *mlc-4*. *nmy-2(RNAi)* did not enhance *nmy-1* mutant phenotypes (Figure 6B), suggesting that the *nmy* genes may be nonredundant in wound closure. Knockdown of nonmuscle myosin light chain *mlc-4(RNAi)* also promoted ring closure (Figures 6A and 6B). Inhibition of nonmuscle myosin did not affect postwounding survival (data not shown). Time-lapse analysis of actin dynamics in *nmy-1(sb115)* mutants (Movie S5) suggested that wound closure was accelerated after knockdown of nonmuscle myosin. Taken together, these results suggest *C. elegans* adult epidermal wounds do not close by a purse-string mechanism.

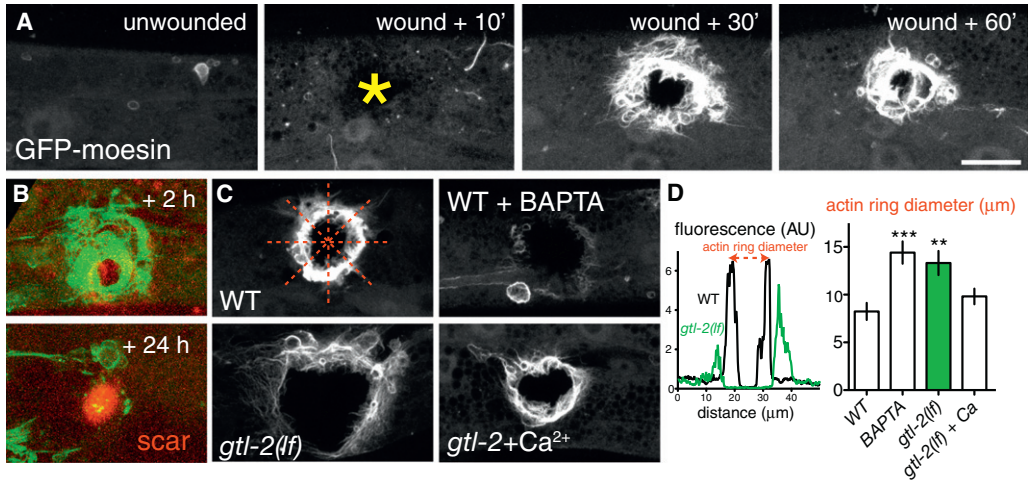

Figure 4. Wounding Triggers Ca^{2+}-Dependent Formation of Actin Rings

(A) Epidermal needle wounds trigger formation of actin rings at the wound margin, visualized with P*col-19*-GFP-moesin (*juIs352*); frames from Movie S4.
(B) In WT animals, actin rings close by 24 hr; an autofluorescent scar (red channel) remains, marking the wound.
(C and D) GFP intensity along line scans of representative WT and *gtl-2(n2618)* mutants; arbitrary units. Quantitation of actin ring diameter from line scans, n > 20 per genotype; four line scans per animal (dotted red lines in C, WT). Statistical comparisons use the Mann-Whitney test. Actin ring assembly and closure is inhibited by incubation in BAPTA-AM and in *gtl-2* mutants. In ~42% of BAPTA-treated animals and 29% of *gtl-2* mutants, the GFP-moesin ring never forms; ring diameters were quantitated in remaining animals. The *gtl-2* actin closure defect is partly suppressed by incubation in buffer containing 2 mM Ca^{2+} ($p = 0.05$).
Scale bars in (A)–(C) represent 10 μm.

Instead, local actin polymerization related to filopodial protrusions appears to be critical.

Loss of DAPK Function Accelerates Wound Closure and Suppresses the Effects of Ca^{2+} Signaling Mutants

The Ca^{2+}-calmodulin-regulated kinase DAPK/DAPK-1 has been shown to negatively regulate epidermal innate immune responses to damage [14] and is a known regulator of nonmuscle myosin [35]. We therefore tested whether DAPK/*dapk-1* might also negatively regulate cytoskeletal dynamics in wound closure. In *dapk-1* single mutants, GFP-moesin rings were smaller than in the WT and closed more rapidly, paralleling the *rho-1* and *nmy-1* phenotypes (Movie S5). To address whether such mutations could overcome the effects of reduced Ca^{2+} signals, we constructed double mutants between *dapk-1* and *gtl-2*, *egl-8*, and *egl-30.* We found that *gtl-2 dapk-1* double mutants displayed significantly faster ring closure than did *gtl-2* mutants (Figures 6A and 6B). *dapk-1* mutants displayed normal epidermal Ca^{2+} dynamics (data not shown). Finally, the low postwound survival of *egl-30*, *egl-8*, or *gtl-2* single and compound mutants was significantly suppressed by *dapk-1(lf)* (Figure 6C). These results support DAPK-1 acting as a negative regulator of wound closure dynamics, either downstream or in parallel to Ca^{2+} signals.

Discussion

In conclusion, we have identified a G protein/Ca^{2+} based wound closure pathway in the adult *C. elegans* epidermis. Our results link single-cell and embryonic wound models to physiologically relevant outcomes in repair of a mature barrier epithelium. Previous work has shown that epidermal immune responses to wounding and fungal infection depend on $G\alpha_{12}$/GPA-12 [26]. We find that $G\alpha_q$/EGL-30 and Ca^{2+} act in parallel to promote epidermal wound closure via actin polymerization (Figures 7A and 7B). Although the $G\alpha_q$-Ca^{2+} pathway described here is not required for upregulation of antimicrobial peptides after wounding, it could play other roles in antimicrobial defense. For example, $G\alpha_q$ and PLCβ regulate insulin secretion and PMK-1 in intestinal innate immunity in *C. elegans* [36]. Clearly, an important future goal is to identify the activators and effectors of $G\alpha_q$ in the epidermis.

Our analysis suggests that at least two sources contribute to epidermal Ca^{2+}, possibly in sequence. The TRPM channel GTL-2 is important for epidermal Ca^{2+} responses, suggesting that wounding triggers an influx of Ca^{2+} via GTL-2. As several studies indicate, GTL-2 localizes to cell plasma membranes rather than internal compartments [21, 22], it might directly sense wound-triggered changes in membrane tension. Alternatively, like other mechanosensitive TRP channels, GTL-2 might be indirectly gated by GPCR signaling [37]. The mechanism of gating of GTL-2 remains an open question. The EGL-30/EGL-8 pathway may be activated by an initial GTL-2-dependent Ca^{2+} influx to trigger further ITR-1-dependent release of Ca^{2+} from intracellular stores. Mammalian epidermal cells express a variety of TRP channels, some of which are implicated in epidermal wound healing [38]. Indeed, application of TRPM agonists can promote barrier reformation after wounding [39], suggesting that some roles of TRPM channels in wound healing may be conserved.

Our results suggest a model for how Ca^{2+} signals trigger wound closure in the adult *C. elegans* epidermis (Figure 7B). CDC-42 is essential for actin rings to form, consistent with findings that Cdc42 is important in *Drosophila* larval wound closure [29]. As Cdc42 is activated by Ca^{2+} after wounding in *Xenopus* oocytes [40], it may act downstream of the Ca^{2+} signal in the *C. elegans* epidermis. Why does actin accumulate locally at wound sites when the Ca^{2+} signal is delocalized? This may be explained if Ca^{2+} acts with a local signal, possibly generated by cellular "compartment mixing" [41]. In contrast, Rho acts antagonistically to CDC-42 in *C. elegans* wound

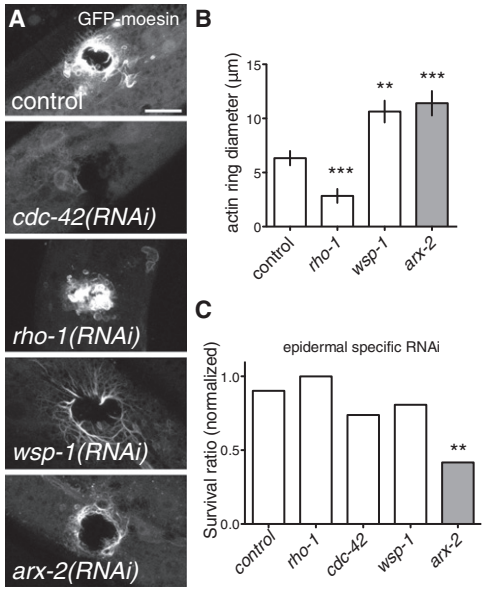

Figure 5. Wound Closure Requires Actin Polymerization Factors and Cdc42 and Is Inhibited by Rho

(A and B) Ring formation is abolished in *cdc-42(RNAi)* animals and promoted in *rho-1(RNAi)* animals (control, L4440 empty vector). Of the three Rac genes, only *mig-2* showed a weak requirement for ring formation (data not shown). Ring closure was reduced after RNAi for *wsp-1*/WASP and *arx-2*/Arp2/3. Scale bar represents10 μm (A).

(C) Survival postwounding is unaffected by *rho-1(RNAi)*, slightly impaired by *cdc-42(RNAi)*, and strongly reduced by *arx-2(RNAi)*. Statistical analysis used t test (C) or Fisher's exact test (B).

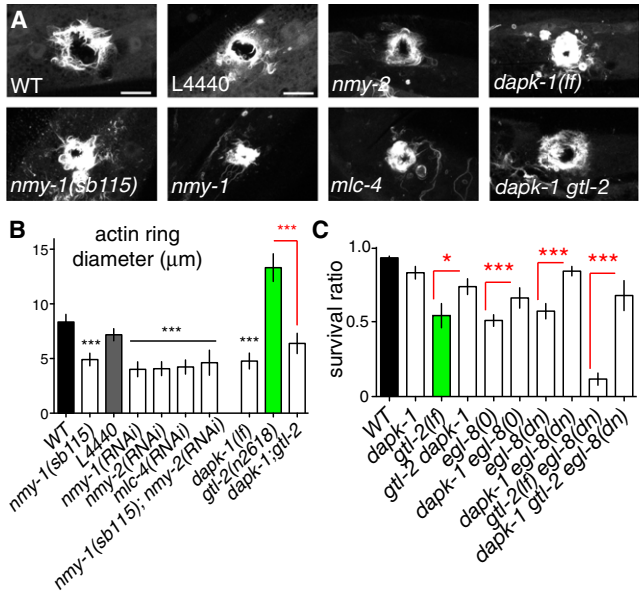

Figure 6. Negative Regulation of Wound Closure by Nonmuscle Myosin and DAPK

(A) Loss of function in nonmuscle myosin and *dapk-1* promotes actin ring closure. GFP-moesin (*juIs352*) imaged at 1 hr postwounding in *nmy-1(sb115)* mutants and after RNAi for *nmy-1, nmy-2, mlc-4* (control: L4440). Survival postwounding was unaffected under these conditions (not shown). Actin ring assembly is enhanced in *dapk-1(ju4)* and in *dapk-1 gtl-2* double mutants (compared *gtl-2* in Figure 4C). Confocal projections of Z stacks, 1 hr post needle wound.

(B) Quantitation of actin ring diameters as in Figure 4.

(C) *dapk-1* suppresses the postwound survival defects of *gtl-2*, *egl-8*, and of *gtl-2 egl-8* double mutants. n > 100 per genotype; Fisher's exact test was used.

responses. Rho and CDC-42 might directly antagonize, as in *Xenopus* oocyte wounding [42]. Alternatively, the enhanced closure seen after inhibition of Rho or nonmuscle myosin might be an indirect consequence of reduced actin cable formation. Future studies should address whether and how Rho and CDC-42 are locally activated at wounds. Nevertheless, our results suggest that, unlike embryonic epithelia in which purse-string actomyosin contractility has a major role, wound closure in the adult *C. elegans* epidermis is driven by directed actin polymerization. The unexpected negative role of nonmuscle myosin suggests that actin cable formation may compete with actin polymerization in wound closure. *C. elegans* wound closure may more resemble that found in other adult epithelia, in which closure is driven by filopodial protrusion at the epithelial leading edge [43]. Most of our wounds affect the large syncytial epidermal cell hyp7, distant from their contacts with other epidermal cells such as seam cells. We therefore believe that actin structures formed after wounding are predominantly generated by hyp7, although contributions from other epidermal cells have not yet been examined.

DAPK-1 is a negative regulator of the innate immune response to wounding [14]. Because DAPK is regulated by Ca^{2+} [44], DAPK-1 is an excellent candidate to be regulated by Ca^{2+} signals reported here. The inhibitory role of DAPK-1 in closure, together with previous evidence that DAPK-1 inhibits the innate immune response to damage, indicates that DAPK-1 acts as a coordinate negative regulator of wound responses. If this inhibitory role for DAPK is conserved, pharmacological inhibition of DAPK could be a promising avenue for acceleration of wound healing.

Experimental Procedures

C. elegans Genetics

All strains were maintained at 20°C–22.5°C on NGM agar plates with *E. coli* OP50 as food source. Strains were constructed using standard procedures, and genotypes confirmed by PCR or sequencing. Mutations used include: *gtl-2[n2618(lf), tm1463(0)]*, *egl-8[n488(dn), sa47(0)]*, *egl-30(n686, ad805, js126gf)*, *itr-1(jc5cs)*, *dapk-1(ju4, gk219)*, *rde-1(ne219)*, *pmk-1(km25)*, *tir-1(tm3036)*, *tpa-1(k501, k530)*, *gpa-12(pk322)*, *gon-2(q365)*, *gtl-1(dx171)*, *nmy-1(sb115)*. New transgenic strains are listed in Table S1.

Needle Wounding, Survival Assay, and Drug Experiments

We wounded animals with single stabs of a microinjection needle to the posterior body 24 hr after L4 stage, as described [13]. We transferred wounded animals to new plates and scored viability every 24 hr; we defined death as failure to respond to touch. In some assays, we prevented bacterial proliferation and egg-laying by transferring animals to plates containing 50 mg/mL FUDR immediately before wounding. Calcium chelators or Latrunculin A were dissolved in dimethyl sulfoxide (DMSO) or M9 and then diluted in M9. We incubated wounded worms in drug solution (containing *E. coli* OP50) and checked survival every 12 hr; control animals were incubated in M9 or DMSO. In experiments where unwounded strains displayed similar survival 24 hr after L4, we calculated normalized survival (fraction surviving 24 hr after wounding)/(fraction surviving unwounded). To image GCaMP after needle wounding on plates, we used a Zeiss Discovery V12 dissecting stereomicroscope and a Nikon DS Qi-1 monochrome camera.

Adult Epidermal-Specific RNAi

To knock down gene expression in the adult epidermis, we expressed the WT RDE-1 gene under the control of P*col-19* (*juIs346*) in an *rde-1(ne219)* mutant background. *rde-1* mutants are resistant to RNAi; because the *col-19* promoter is expressed only in late L4 and adult epidermis, transgenic animals are resistant to RNAi in all tissues except the adult epidermis. We

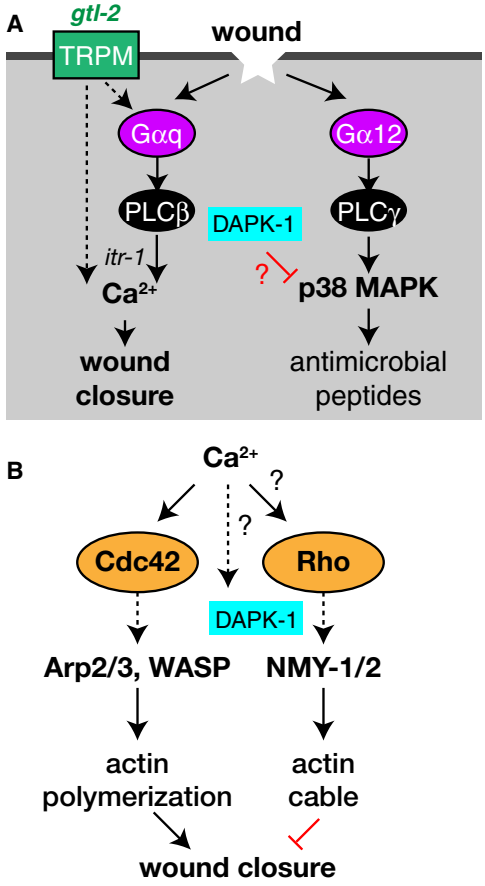

Figure 7. Wound Response Pathways in the Adult *C. elegans* Epidermis

(A) Model for the relationship of the innate immunity and wound closure pathways in *C. elegans* epidermal wound repair.

(B) Possible mechanism of small GTPase regulation in wound healing.

transferred *rde-1; Pcol-19-RDE-1(juIs346)* as L1s to bacteria expressing appropriate double-stranded RNA (dsRNA), wounded the animals as day 1 adults, and assayed survival after 24 hr. Other (tissue-nonspecific) RNAi experiments were performed in a similar way, with animals grown from the L1 stage on RNAi bacteria and wounded as young adults. Feeding RNAi clones were obtained from the Ahringer library and confirmed by sequencing or made by PCR from cDNA or genomic templates; a complete list of RNAi clones is available on request.

Laser Wounding and Imaging

To analyze epidermal Ca^{2+}, we wounded animals using femtosecond laser irradiation, essentially as described [45] except with 2 × 200 ms pulses. We imaged GCaMP fluorescence using spinning disk confocal microscopy, as described [45]. For short movies (<30 s) we acquired a single channel in burst mode; for longer time-lapse series, we acquired two channels every 30–60 s. To measure peak $\Delta F/F_0$, we imaged ten frames using a 100X objective (Zeiss Planapo, N.A. 1.46). We measured average fluorescence in ten equivalent regions of interest (ROI), five centered on the epidermal cell and five in the background. Baseline fluorescence (F_0) was obtained by averaging fluorescence in five ROIs in the epidermis then subtracting the average of 5 ROIs in the background before injury. GCaMP fluorescence was normalized to an internal control, P*col-19*-tdTomato; tdTomato or GFP levels did not change after wounding (Figure S1B). The change in fluorescence ΔF was expressed as the ratio of change with respect to the baseline $[(F_t-F_0)/F_0]$. To follow $\Delta F/F_0$ over time at different distances from the injury site, we imaged using the 63X objective and drew 2 μm ROIs at intervals of 5 μm. As the GCaMP transient extended 10 μm from the injury site within 230 ms of wounding, we selected a 10 μm long ROI to compare initial $\Delta F/F_0$ between conditions.

To quantitate epidermal GFP-moesin (*juIs352*), we used confocal microscopy to acquire Z stacks (13 × 0.5 μm) of GFP-moesin rings after wounding. We generated maximum intensity projections of each Z stack. For each image we used four line scans (oriented at 45° to each other) over the GFP-moesin ring and defined actin ring diameter as the average peak to peak distance. In some conditions (e.g., BAPTA-AM, *gtl-2*) a significant fraction of animals did not assemble GFP-moesin rings after wounding; such animals were not included in quantitation. In cases where the actin ring had closed by 1 hr we defined the diameter as 0. In embryonic epidermis GFP-moesin localized to circumferential bundles (not shown), consistent with known distribution of F-actin.

Statistical Analysis

All statistical analyses used GraphPad Prism (La Jolla, CA). Two-way comparisons used the Student's t test, Mann-Whitney test, or Fisher's exact test for proportions.

Supplemental Information

Supplemental Information includes three figures, two tables, Supplemental Experimental Procedures, and five movies and can be found with this article online at doi:10.1016/j.cub.2011.10.050.

Acknowledgments

We thank Amy Tong for initial work on the epidermal calcium sensor, Tiffany Hsiao for help with transgene integration and mapping, Zilu Wu for assistance with the femtosecond laser, Claudiu Giurumescu for help with confocal imaging, and Anindya Ghosh-Roy for constructs and advice on GCaMP imaging. We thank Loren Looger for GCaMP3, Arshad Desai and Fabio Piano for the moesin clone, Emily Troemel for use of her real-time PCR machine, and Tamara Stawicki and Yishi Jin for sharing information and reagents prior to publication. We thank Yishi Jin, Bill McGinnis, Karen Oegema, Emily Troemel, Nathalie Pujol, Jonathan Ewbank, and members of the Jin and Chisholm laboratories for discussions and comments on this manuscript. This work was supported by National Institutes of Health grant R01 GM54657 to A.D.C.

Received: July 10, 2011
Revised: October 2, 2011
Accepted: October 27, 2011
Published online: November 17, 2011

References

1. Gurtner, G.C., Werner, S., Barrandon, Y., and Longaker, M.T. (2008). Wound repair and regeneration. Nature *453*, 314–321.
2. Sen, C.K., Gordillo, G.M., Roy, S., Kirsner, R., Lambert, L., Hunt, T.K., Gottrup, F., Gurtner, G.C., and Longaker, M.T. (2009). Human skin wounds: a major and snowballing threat to public health and the economy. Wound Repair Regen. *17*, 763–771.
3. Martin, P. (1997). Wound healing—aiming for perfect skin regeneration. Science *276*, 75–81.
4. Schäfer, M., and Werner, S. (2007). Transcriptional control of wound repair. Annu. Rev. Cell Dev. Biol. *23*, 69–92.
5. Galko, M.J., and Krasnow, M.A. (2004). Cellular and genetic analysis of wound healing in *Drosophila* larvae. PLoS Biol. *2*, E239.
6. Mace, K.A., Pearson, J.C., and McGinnis, W. (2005). An epidermal barrier wound repair pathway in Drosophila is mediated by grainy head. Science *308*, 381–385.
7. Ting, S.B., Caddy, J., Hislop, N., Wilanowski, T., Auden, A., Zhao, L.L., Ellis, S., Kaur, P., Uchida, Y., Holleran, W.M., et al. (2005). A homolog of Drosophila grainy head is essential for epidermal integrity in mice. Science *308*, 411–413.
8. Wang, S., Tsarouhas, V., Xylourgidis, N., Sabri, N., Tiklová, K., Nautiyal, N., Gallio, M., and Samakovlis, C. (2009). The tyrosine kinase Stitcher activates Grainy head and epidermal wound healing in Drosophila. Nat. Cell Biol. *11*, 890–895.
9. Wu, Y., Brock, A.R., Wang, Y., Fujitani, K., Ueda, R., and Galko, M.J. (2009). A blood-borne PDGF/VEGF-like ligand initiates wound-induced epidermal cell migration in Drosophila larvae. Curr. Biol. *19*, 1473–1477.
10. Werner, S., and Grose, R. (2003). Regulation of wound healing by growth factors and cytokines. Physiol. Rev. *83*, 835–870.

11. Luo, H., Liu, Y., Fang, L., Li, X., Tang, N., and Zhang, K. (2007). *Coprinus comatus* damages nematode cuticles mechanically with spiny balls and produces potent toxins to immobilize nematodes. Appl. Environ. Microbiol. *73*, 3916–3923.
12. Glockling, S.L., and Beakes, G.W. (2000). An ultrastructural study of sporidium formation during infection of a rhabditid nematode by large gun cells of *Haptoglossa heteromorpha*. J. Invertebr. Pathol. *76*, 208–215.
13. Pujol, N., Cypowyj, S., Ziegler, K., Millet, A., Astrain, A., Goncharov, A., Jin, Y., Chisholm, A.D., and Ewbank, J.J. (2008). Distinct innate immune responses to infection and wounding in the *C. elegans* epidermis. Curr. Biol. *18*, 481–489.
14. Tong, A., Lynn, G., Ngo, V., Wong, D., Moseley, S.L., Ewbank, J.J., Goncharov, A., Wu, Y.C., Pujol, N., and Chisholm, A.D. (2009). Negative regulation of *Caenorhabditis elegans* epidermal damage responses by death-associated protein kinase. Proc. Natl. Acad. Sci. USA *106*, 1457–1461.
15. Stanisstreet, M. (1982). Calcium and wound healing in *Xenopus* early embryos. J. Embryol. Exp. Morphol. *67*, 195–205.
16. McNeil, P.L., and Steinhardt, R.A. (2003). Plasma membrane disruption: repair, prevention, adaptation. Annu. Rev. Cell Dev. Biol. *19*, 697–731.
17. Nodder, S., and Martin, P. (1997). Wound healing in embryos: a review. Anat. Embryol. (Berl.) *195*, 215–228.
18. Tian, L., Hires, S.A., Mao, T., Huber, D., Chiappe, M.E., Chalasani, S.H., Petreanu, L., Akerboom, J., McKinney, S.A., Schreiter, E.R., et al. (2009). Imaging neural activity in worms, flies and mice with improved GCaMP calcium indicators. Nat. Methods *6*, 875–881.
19. Walker, D.S., Gower, N.J., Ly, S., Bradley, G.L., and Baylis, H.A. (2002). Regulated disruption of inositol 1,4,5-trisphosphate signaling in *Caenorhabditis elegans* reveals new functions in feeding and embryogenesis. Mol. Biol. Cell *13*, 1329–1337.
20. Kahn-Kirby, A.H., and Bargmann, C.I. (2006). TRP channels in *C. elegans*. Annu. Rev. Physiol. *68*, 719–736.
21. Stawicki, T.M., Zhou, K., Yochem, J., Chen, L., and Jin, Y. (2011). TRPM channels modulate epileptic-like convulsions via systemic ion homeostasis. Curr. Biol. *21*, 883–888.
22. Teramoto, T., Sternick, L.A., Kage-Nakadai, E., Sajjadi, S., Siembida, J., Mitani, S., Iwasaki, K., and Lambie, E.J. (2010). Magnesium excretion in *C. elegans* requires the activity of the GTL-2 TRPM channel. PLoS ONE *5*, e9589.
23. Couillault, C., Pujol, N., Reboul, J., Sabatier, L., Guichou, J.F., Kohara, Y., and Ewbank, J.J. (2004). TLR-independent control of innate immunity in *Caenorhabditis elegans* by the TIR domain adaptor protein TIR-1, an ortholog of human SARM. Nat. Immunol. *5*, 488–494.
24. Bastiani, C.A., Gharib, S., Simon, M.I., and Sternberg, P.W. (2003). Caenorhabditis elegans Galphaq regulates egg-laying behavior via a PLCβ-independent and serotonin-dependent signaling pathway and likely functions both in the nervous system and in muscle. Genetics *165*, 1805–1822.
25. Zugasti, O., and Ewbank, J.J. (2009). Neuroimmune regulation of antimicrobial peptide expression by a noncanonical TGF-β signaling pathway in *Caenorhabditis elegans* epidermis. Nat. Immunol. *10*, 249–256.
26. Ziegler, K., Kurz, C.L., Cypowyj, S., Couillault, C., Pophillat, M., Pujol, N., and Ewbank, J.J. (2009). Antifungal innate immunity in C. elegans: PKCδ links G protein signaling and a conserved p38 MAPK cascade. Cell Host Microbe *5*, 341–352.
27. Martin, P., and Lewis, J. (1992). Actin cables and epidermal movement in embryonic wound healing. Nature *360*, 179–183.
28. Wood, W., Jacinto, A., Grose, R., Woolner, S., Gale, J., Wilson, C., and Martin, P. (2002). Wound healing recapitulates morphogenesis in *Drosophila* embryos. Nat. Cell Biol. *4*, 907–912.
29. Lesch, C., Jo, J., Wu, Y., Fish, G.S., and Galko, M.J. (2010). A targeted UAS-RNAi screen in *Drosophila* larvae identifies wound closure genes regulating distinct cellular processes. Genetics *186*, 943–957.
30. Clark, A.G., Miller, A.L., Vaughan, E., Yu, H.Y., Penkert, R., and Bement, W.M. (2009). Integration of single and multicellular wound responses. Curr. Biol. *19*, 1389–1395.
31. Edwards, K.A., Demsky, M., Montague, R.A., Weymouth, N., and Kiehart, D.P. (1997). GFP-moesin illuminates actin cytoskeleton dynamics in living tissue and demonstrates cell shape changes during morphogenesis in Drosophila. Dev. Biol. *191*, 103–117.
32. Brock, J., Midwinter, K., Lewis, J., and Martin, P. (1996). Healing of incisional wounds in the embryonic chick wing bud: characterization of the actin purse-string and demonstration of a requirement for Rho activation. J. Cell Biol. *135*, 1097–1107.
33. Nobes, C.D., and Hall, A. (1995). Rho, rac, and cdc42 GTPases regulate the assembly of multimolecular focal complexes associated with actin stress fibers, lamellipodia, and filopodia. Cell *81*, 53–62.
34. Piekny, A.J., Johnson, J.L., Cham, G.D., and Mains, P.E. (2003). The *Caenorhabditis elegans* nonmuscle myosin genes *nmy-1* and *nmy-2* function as redundant components of the *let-502*/Rho-binding kinase and *mel-11*/myosin phosphatase pathway during embryonic morphogenesis. Development *130*, 5695–5704.
35. Bialik, S., Bresnick, A.R., and Kimchi, A. (2004). DAP-kinase-mediated morphological changes are localization dependent and involve myosin-II phosphorylation. Cell Death Differ. *11*, 631–644.
36. Kawli, T., Wu, C., and Tan, M.W. (2010). Systemic and cell intrinsic roles of Gqα signaling in the regulation of innate immunity, oxidative stress, and longevity in Caenorhabditis elegans. Proc. Natl. Acad. Sci. USA *107*, 13788–13793.
37. Christensen, A.P., and Corey, D.P. (2007). TRP channels in mechanosensation: direct or indirect activation? Nat. Rev. Neurosci. *8*, 510–521.
38. Yamada, T., Ueda, T., Ugawa, S., Ishida, Y., Imayasu, M., Koyama, S., and Shimada, S. (2010). Functional expression of transient receptor potential vanilloid 3 (TRPV3) in corneal epithelial cells: involvement in thermosensation and wound healing. Exp. Eye Res. *90*, 121–129.
39. Denda, M., Tsutsumi, M., and Denda, S. (2010). Topical application of TRPM8 agonists accelerates skin permeability barrier recovery and reduces epidermal proliferation induced by barrier insult: role of cold-sensitive TRP receptors in epidermal permeability barrier homoeostasis. Exp. Dermatol. *19*, 791–795.
40. Benink, H.A., and Bement, W.M. (2005). Concentric zones of active RhoA and Cdc42 around single cell wounds. J. Cell Biol. *168*, 429–439.
41. Bement, W.M., Yu, H.Y., Burkel, B.M., Vaughan, E.M., and Clark, A.G. (2007). Rehabilitation and the single cell. Curr. Opin. Cell Biol. *19*, 95–100.
42. Vaughan, E.M., Miller, A.L., Yu, H.Y., and Bement, W.M. (2011). Control of local Rho GTPase crosstalk by Abr. Curr. Biol. *21*, 270–277.
43. Sonnemann, K.J., and Bement, W.M. (2011). Wound repair: toward understanding and integration of single-cell and multicellular wound responses. Annu. Rev. Cell Dev. Biol. *27*, 237–263.
44. Bialik, S., and Kimchi, A. (2006). The death-associated protein kinases: structure, function, and beyond. Annu. Rev. Biochem. *75*, 189–210.
45. Ghosh-Roy, A., Wu, Z., Goncharov, A., Jin, Y., and Chisholm, A.D. (2010). Calcium and cyclic AMP promote axonal regeneration in *Caenorhabditis elegans* and require DLK-1 kinase. J. Neurosci. *30*, 3175–3183.